Effect of zinc oxide nanoparticles as cure activator on the properties of natural rubber and nitrile rubber

ARTICLE *in* JOURNAL OF APPLIED POLYMER SCIENCE · AUGUST 2007

Impact Factor: 1.77 · DOI: 10.1002/app.26296

5 AUTHORS, INCLUDING:

Suchismita Sahoo
Guru Gobind Singh Indraprastha University
4 PUBLICATIONS **86** CITATIONS
SEE PROFILE

Madhuchhanda Maiti
Reliance Industries Limited
31 PUBLICATIONS **597** CITATIONS
SEE PROFILE

Anirban Ganguly
Saudi Basic Industries Corporation (SABIC)
13 PUBLICATIONS **228** CITATIONS
SEE PROFILE

Jinu George
Rubber Research Institute of India
13 PUBLICATIONS **163** CITATIONS
SEE PROFILE

Effect of Zinc Oxide Nanoparticles as Cure Activator on the Properties of Natural Rubber and Nitrile Rubber

Suchismita Sahoo, Madhuchhanda Maiti, Anirban Ganguly, Jinu Jacob George, Anil K. Bhowmick

Rubber Technology Centre, Indian Institute of Technology, Kharagpur, 721 302, India

Received 17 September 2006; accepted 8 February 2007
DOI 10.1002/app.26296
Published online 8 May 2007 in Wiley InterScience (www.interscience.wiley.com).

ABSTRACT: Zinc oxide (ZnO) nanoparticles were synthesized by homogeneous precipitation and calcination method and were then characterized by transmission electron microscopy and X-ray diffraction analysis. Synthesized ZnO was found to have no impurity and had a dimension ranging from 30–70 nm with an average of 50 nm. The effect of these ZnO nanoparticles as cure activator was studied for the first time in natural rubber (NR) and nitrile rubber (NBR) and compared with conventional rubber grade ZnO with special reference to mechanical and dynamic mechanical properties. From the rheograph, the maximum torque value was found to increase for both NR and NBR compounds containing ZnO nanoparticles. ZnO nanoparticles were found to be more uniformly dispersed in the rubber matrix in comparison with the conventional rubber grade ZnO as evident from scanning electron microscopy/X-ray dot mapping analysis. The tensile strength was observed to improve by 80% for NR when ZnO nanoparticles were used as cure activator instead of conventional rubber grade ZnO. An improvement of 70% was observed in the case of NBR. The glass transition temperature (T_g) showed a positive shift by 6°C for both NR and NBR nanocomposites, which indicated an increase in crosslinking density. The swelling ratio was found to decrease in the case of both NR and NBR, and volume fraction of rubber in swollen gel was observed to increase, which supported the improvement in mechanical and dynamic mechanical properties. J Appl Polym Sci 105: 2407–2415, 2007

Key words: ZnO nanoparticles; cure activator; natural rubber; nitrile rubber; cure characteristics; mechanical properties and dynamic mechanical properties

INTRODUCTION

Zinc oxide (ZnO) is an important inorganic pigment for the rubber industry, and over the past 100 years, rubber industry has utilized an increasing number of physical and chemical properties of ZnO.[1] ZnO is manufactured industrially by the French and the American processes. In the French process, pure metal is evaporated to obtain a pure oxide, whereas in the American process zinc oxide is obtained directly from a zinc ore by burning it with coal or electro thermally. The conventional rubber grade ZnO has particle size ranging from 0.1 to 0.4 μm and a corresponding specific surface area in the range of 10–20 m^2/g.[2] ZnO finds wide application because of its photochemical properties and chemical reactivity. ZnO has proved to be the most cost effective inorganic pigment to activate the rate of sulfur cure with the accelerators. The reaction mechanism for the cure activation is represented in Scheme 1.[3] ZnO is also widely used as a UV stabilizer and as an additive having biocidal activity. Remaining in the invisible form in the finished product, zinc has long been used as an essential compounding ingredient in rubber. It was one of the first pigments extensively used in the rubber products manufacturing. The first published reference to such application is in a patent[4] granted in 1849.

For better heat conductivity and reinforcement in heavy-duty pneumatic tires, high loadings of zinc oxide are used, since heat-buildup is a critical problem at their higher operating speeds. But some adverse environmental effects of zinc exposure have been reported, which include decline in earthworm population densities, species diversity and the development of tolerant grass species.[5] The main sources of zinc pollution are iron and steel production, nonferrous metals manufacture, road transport, and to a lesser extent coal combustion. The road transport emission is almost entirely because of tire wear. This arises from the zinc content of the tire rubber—around 2% ZnO by weight.[5] For many of its uses, there is currently no other economic alternative at present. Hence, ZnO nanoparticles might help in reducing the level of ZnO in conventional formulations.

There are several different methods available in the literature to synthesize ZnO nanoparticles such as high temperature solid–vapor deposition,[6] solution phase methods,[7] colloidal chemistry techniques,[8] sol-gel method,[9,10] phase transfer technique,[11] hydro-

Correspondence to: A. K. Bhowmick (anilkb@rtc.iitkgp.ernet.in).

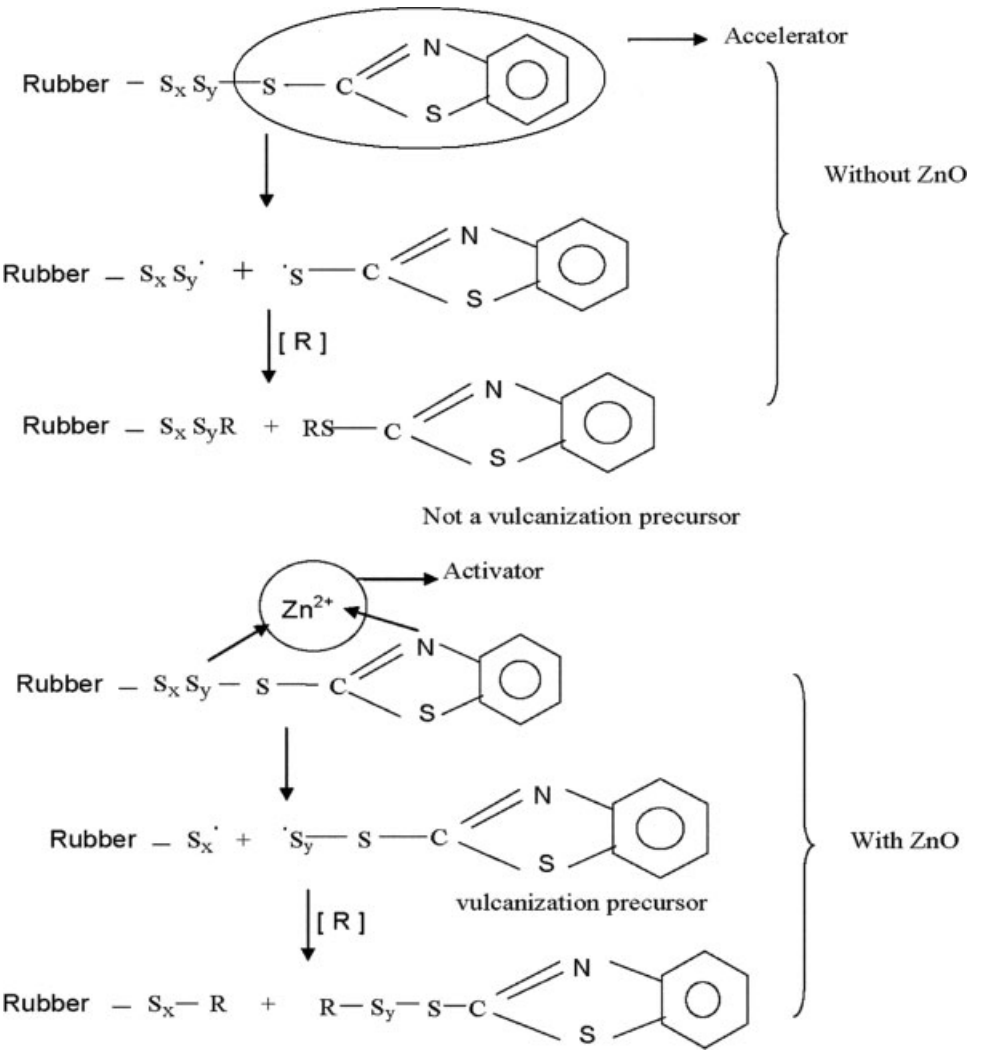

Scheme 1 Cure reaction mechanism in the presence of activator (ZnO) and in the absence of ZnO.[3]

lysis of chelate complex,[12] polymer stabilization,[13–15] synthesis in reversed micelles,[16] alkoxide based process,[17] precipitation method,[18] microemulsion,[16,19,20] spray pyrolysis,[21–23] hydrothermal method,[24,25] laser vaporization condensation,[26] and flow injection synthesis.[27] In the present study, the precipitation method has been used for synthesizing ZnO nanoparticles. Commonly, the precipitation technique needs calcination of the precipitation precursor and is the simplest method of synthesizing ZnO nanoparticles in the laboratory. For ZnO nanoparticles, the surface area is higher because of reduction in size, as ZnO has little porosity.

Numerous researchers have already worked on the effect of different nanofillers like clay and silica.[28–32] The effect of nanosilica has also been investigated by Bandopadhyay et.al from our laboratory.[33,34] The effect of nanoclay has also been explored extensively in our laboratory.[35–37] The effect of ZnO nanoparticles as curing agent has also been studied.[38,39]

Hence, the aim of the present study is to investigate the effect of ZnO nanoparticles as *cure activator* in natural rubber (NR) and nitrile rubber (NBR), since these are the most widely used elastomers in a variety of applications. NR finds use in tires, mechanical goods, engineering products, whereas NBR finds applications, where fuel and oil resistance is the primary requirement.[40] The present study is focused on the effect of ZnO nanoparticles as cure activator in NR and NBR and the results are compared with conventional rubber grade ZnO, at different loadings of ZnO.

EXPERIMENTAL

Synthesis of zinc oxide nanoparticles

Materials

Laboratory grade zinc nitrate hexahydrate [Zn $(NO_3)_2 \cdot 6H_2O$], ammonium carbonate [$(NH_4)_2CO_3$] and ethanol were purchased from Merck (I), Mumbai.

TABLE I
Formulation and Compound Designation for NR

Compound designation	NR-RG	NR-N5	NR-N3
Formulation			
NR	100	100	100
ZnO	5.0	5.0	3.0
Stearic acid	2.0	2.0	2.0
Antioxidant (TQ)	2.0	2.0	2.0
CBS	0.8	0.8	0.8
TMTD	0.2	0.2	0.2
Sulphur	2.5	2.5	2.5
ZnO used	Rubber grade	ZnO nanoparticles	ZnO nanoparticles

All weights are in parts per hundred grams of rubber.
TQ, 2,2,4-trimethyl-1,2-dihydroquinoline; CBS, *N*-cyclohexylbenzothiazole-2-sulphenamide; TMTD, tetramethyl thiuram disulfide.

Method of synthesis

$Zn(NO_3)_2 \cdot 6H_2O$ and $(NH_4)_2CO_3$ were, respectively, dissolved in distilled water at a concentration of 1.0*M*. $Zn(NO_3)_2$ solution was then slowly dropped into the vigorously stirred $(NH_4)_2CO_3$ solution with a molar ratio of 1 : 2 to prepare the precursor. A white precipitate occurred immediately when the two solutions mixed with each other, but it dissolved with stirring. A stable state slowly occurred because of the high concentration of Zn^{2+} ions. The solid was collected by filtration, repeatedly rinsed with ethanol, and then dried at 100°C for 12 h. ZnO nanoparticles were obtained after calcination at 280°C. This method was very similar to that reported by Wang and Gao.[41]

Characterization

The synthesized ZnO nanoparticles were characterized by transmission electron microscopy (TEM, JEOL 2010). The samples were dispersed in acetone by ultrasonic bath and a drop of it was deposited on carbon-coated copper grid and was analyzed under an accelerating voltage of 200 kV.

X-ray diffraction studies were done using Rigaku CN2005 X-ray Diffractometer ''Miniflex'' model in the range of 10° to 50° (= 2θ). The zinc oxide powder was deposited on the sample holder uniformly. The Joint Committee of Powder Diffraction Studies (JCPDS) maintains a database of diffraction patterns, including the *d*-spacing. These were used to identify the peaks obtained in the XRD of ZnO nanoparticles.

Preparation and characterization of rubber composite

Compounding and vulcanization

The compounds were mixed as per the formulations given in Tables I and II in a laboratory two-roll open mixing mill at a friction ratio 1 : 1.2. The rolls were cooled to room temperature by continuous circulation of water. The curing studies were followed with an oscillating disc rheometer (Monsanto model 100S) at a temperature of 150°C and oscillating arc of 3°.

The cure rate index, was calculated from the following expression

$$\mathrm{CRI} = 100/(t_{90} - t_2) \quad (1)$$

where t_{90} is the optimum cure time, which is the time corresponding to the torque value calculated using the expression, $M_l + 0.9(M_h - M_l)$, M_h and M_l being the maximum and minimum torque values respectively, and t_2 is the scorch time corresponding

TABLE II
Formulation and Compound Designation for NBR

Compound designation	NBR-RG	NBR-N5	NBR-N3
Formulation			
NBR	100	100	100
Sulphur	1.5	1.5	1.5
ZnO	5	5	3
Stearic acid	1.5	1.5	1.5
Antioxidant (TQ)	1.5	1.5	1.5
MBTS	1.5	1.5	1.5
ZnO used	Rubber grade	ZnO nanoparticles	ZnO nanoparticles

All weights are in parts per hundred grams of rubber.
TQ, 2,2,4-trimethyl-1,2-dihydroquinoline; MBTS, mercapto benzothiazyl disulfide.

to 2-units rise in torque above the minimum torque value.

Reversion time, the time to reach 98% of the maximum torque value after passing through the maxima, was also calculated from the rheograph.

The rubber compounds were cured in a hydraulic press at 150°C for the optimum cure time.

Scanning electron microscopy studies

The dispersion of zinc oxide in the rubber matrix was studied by using JEOL JSM-5800 scanning electron microscope (SEM) operating at an accelerating voltage of 20 kV. The molded samples were sputter coated with gold. For X-ray dot mapping analysis, the photographs were taken at 200 magnifications.

Mechanical properties

Tensile specimens were punched out from the compression molded sheets using ASTM Die-C. The tests were carried out as per ASTM D 412-98 method in a Universal Testing Machine (Hounsfield 10KS) at a crosshead speed of 500 mm/min at room temperature. Three samples were tested and the results were averaged. Their standard deviation was also calculated.

Dynamic mechanical thermal analysis

The dynamic mechanical thermal analysis of the rubber composites with nanozinc oxide and conventional rubber grade zinc oxide were carried out by using a DMTA IV, (Rheometric Scientific, NJ) dynamic mechanical thermal analyzer. The sample specimens were analyzed in tensile mode at a constant frequency of 1 Hz, at 0.01% strain and in the temperature range of −70 to 30°C at a heating rate of 2°C/min. The data were analyzed by RSI Orchestrator application software on an ACER computer attached to the machine. Storage modulus (E'), loss modulus (E''), and loss tangent (tan δ) were measured as a function of temperature for all the representative samples under identical conditions. The temperature corresponding to tan δ peak was taken as the glass transition temperature (T_g).

Swelling studies

A test piece weighing about 0.2 g was punched out from compression-molded sheet. The sample was immersed in toluene for 72 h at room temperature. After 72 h, the test piece was taken out and the swollen weight was taken immediately after removing the adhered surface liquid by a filter paper. The sample was dried in vacuum to constant weight and desorbed weight was taken. The swelling ratio (SR) is defined as

$$\mathrm{SR} = (W_1 - W_0)/W_0 \tag{2}$$

where W_0 is the weight of the test piece before swelling and W_1 is the weight of the swollen test piece. The volume fraction of the rubber in the swollen gel (V_r) was calculated by using the following equation[42]

$$V_r = \frac{[(D - FW_0)\rho_r^{-1}]}{[(D - FW_0)\rho_r^{-1}] + A_0\rho_s^{-1}} \tag{3}$$

where, D, deswollen weight; F, fraction insoluble; W_0, initial weight; A_0, amount of solvent imbibed; ρ_r, density of rubber; and ρ_s, density of solvent.

Degree of crosslinking is a function of SR and volume fraction of rubber in the swollen gel (V_r).

RESULTS AND DISCUSSION

Characterization of ZnO nanoparticles

Figure 1(a) illustrates the TEM micrograph of the synthesized ZnO nanoparticles. The particle size varies from 30 to 70 nm with an average particle size of 50 nm [Fig. 1(b)]. The synthesized ZnO nanoparticles are observed to exhibit slight variations in morphology. As observed from the TEM image in Figure 1(a) which is the representative of a number of TEM images, the particles are polyhedral and spherical in shape.

Figure 2(a,b) shows the X-ray diffractograms of the zinc oxide nanoparticles and the rubber grade ZnO, respectively. All the peaks obtained can be well indexed to the zincite phase of zinc oxide. Both the rubber grade ZnO and the synthesized ZnO nanoparticles give peaks at approximately similar positions, which are in accord with the literature values (JCPDS Card No. 36-1451).[43] Hence, no noticeable change in the crystallographic patterns is observed. The peak heights for the synthesized ZnO nanoparticles are higher due to the reduction in size to nanometers.

The average crystallite size was calculated by using Scherrer equation,[44] i.e.

$$C_s = \frac{K\lambda}{\beta\cos\theta} \tag{4}$$

where β is the integral half-width, K is a constant approximately equal to unity, λ is the wavelength of the incident X-ray (λ = 0.154 nm), C_s is the crystallite size, and θ is the Bragg angle.

The average crystallite size was calculated to be 3.78 nm for the synthesized ZnO nanoparticles,

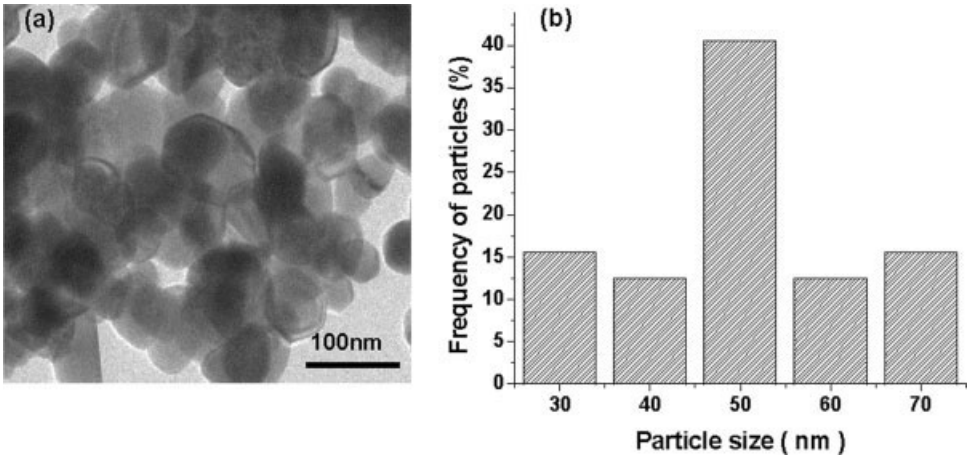

Figure 1 (a) TEM micrograph of ZnO nanoparticle and (b) particle size distribution.

whereas it was 5.00 nm for the rubber grade ZnO. It should be noted that crystallite size is assumed to be the size of a coherently diffracting domain. It is not necessarily the same as particle size.[44]

Properties of the rubber compounds containing ZnO

Dispersion

The dispersion of ZnO nanoparticles was observed to be more uniform in comparison with the conventional rubber grade ZnO as evident from the SEM/X-ray dot mapping analysis shown in Figure 3. Because of reduction in size and increase in the surface area of the ZnO nanoparticles, they effectively form the complex with accelerator, sulfur, and rubber and get easily dispersed into the matrix instead of forming agglomerates on the surface, whereas some agglomerations are observed in the case of conventional rubber grade ZnO [Fig. 3(a)]. Similar observations are also made in the case of NBR, which is not shown here.

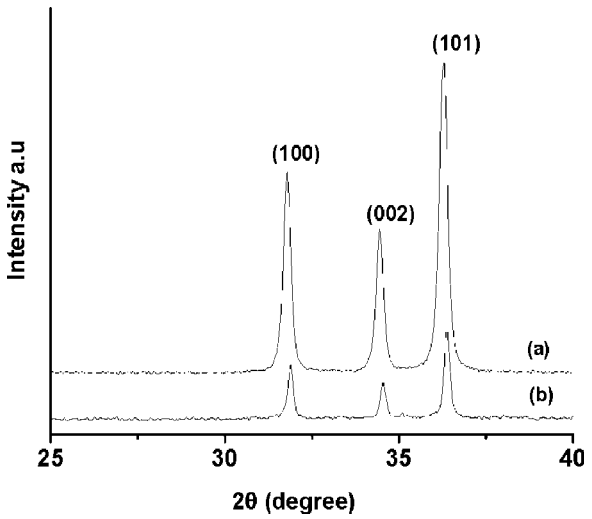

Figure 2 XRD patterns of ZnO nanoparticles synthesized at (a) $C_Z = C_N = 1.0M$, $R_m = 1:2$. (b) XRD pattern of conventional rubber grade ZnO, where C_Z and C_N denote the concentration of zinc nitrate and ammonium carbonate, respectively, and R_m denotes the molar ratio of zinc nitrate to ammonium carbonate solution.

Cure characteristics

Natural rubber. The cure curves are shown in Figure 4(a) and the cure parameters are tabulated in Table III. The maximum torque value shows an improvement by $\sim$ 12% for both 5 and 3 phr loading of ZnO nanoparticles in comparison with the conventional rubber grade ZnO, which indicates a better state of cure because of better interaction of ZnO nanoparticles with the matrix. This may be ascribed to an increase of surface area of the nanoparticles. The difference in maximum and minimum torque value is also improved by 12%, indicating an improvement in modulus and hence the crosslink density. Due to the decrease in dimension of ZnO, the area of con-

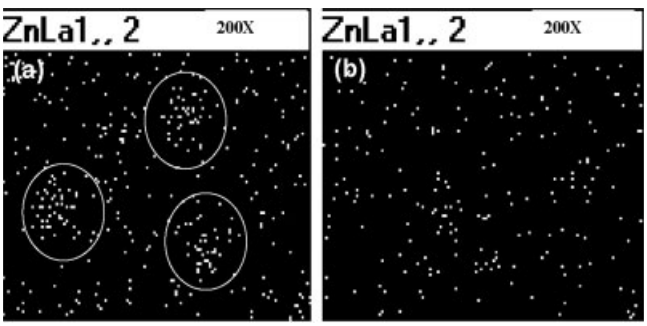

Figure 3 SEM/X-ray dot mapping of (a) NR vulcanizate with conventional rubber grade ZnO, (b) NR vulcanizate (NR-N5)with ZnO nanoparticle showing dispersion of Zn ($\times$200).

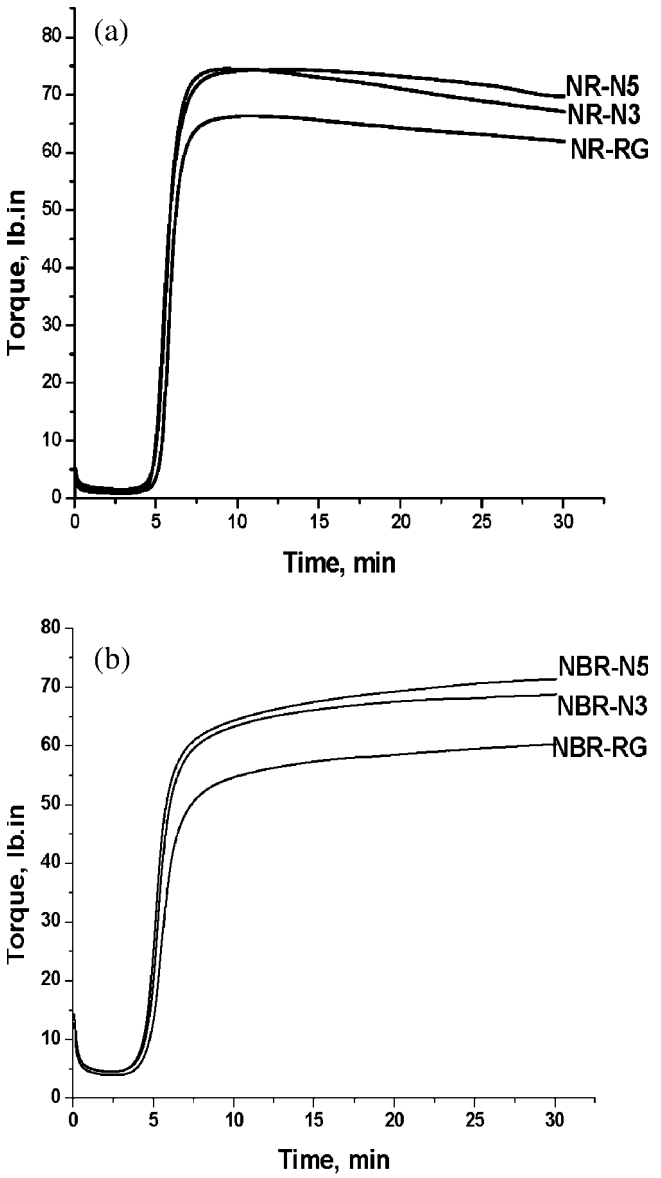

Figure 4 (a) Cure curves for NR compounds, (b) cure curves for NBR compounds.

tact increases which results in the improvement of the maximum torque value. The optimum cure time and the scorch time remain almost unaffected. The reversion time is observed to improve by ~ 25% for NR-N5 in comparison with NR-RG. ZnO makes the elastomer heat resistant. When ZnO nanoparticles are used instead of conventional rubber grade ZnO, the heat resistance of the rubber compound increases, preventing the rubber (NR) from degradation, indicating an improvement in thermal stability of the rubber compound. In the case of NR-N3, there is a slight decrease in reversion time which may be because of decrease in zinc content in the compound. Since the scorch time and the optimum cure

TABLE III
Cure Characteristics of NR Compounds

	NR-RG	NR-N5	NR-N3
Maximum torque (M_h, lb in.)	66.4	74.3	73.9
$M_h - M_l$ (lb in.)	65.3	73.5	73.0
Scorch time (min)	5.0	4.6	4.6
Cure time (min)	6.8	6.7	6.6
Reversion time (min)	15.7	19.4	13.8
Cure rate index (% min^{-1})	55.5	47.6	50.0

TABLE IV
Cure Characteristics of NBR Compounds

	NBR-RG	NBR-N5	NBR-N3
Maximum torque (M_h, lb in.)	60.3	71.4	68.7
$M_h - M_l$ (lb in.)	56.4	67.0	64.2
Scorch time (min)	4.2	3.9	4.0
Cure time (min)	10.0	10.4	9.0
Cure rate index (% min^{-1})	17.1	15.3	20.0

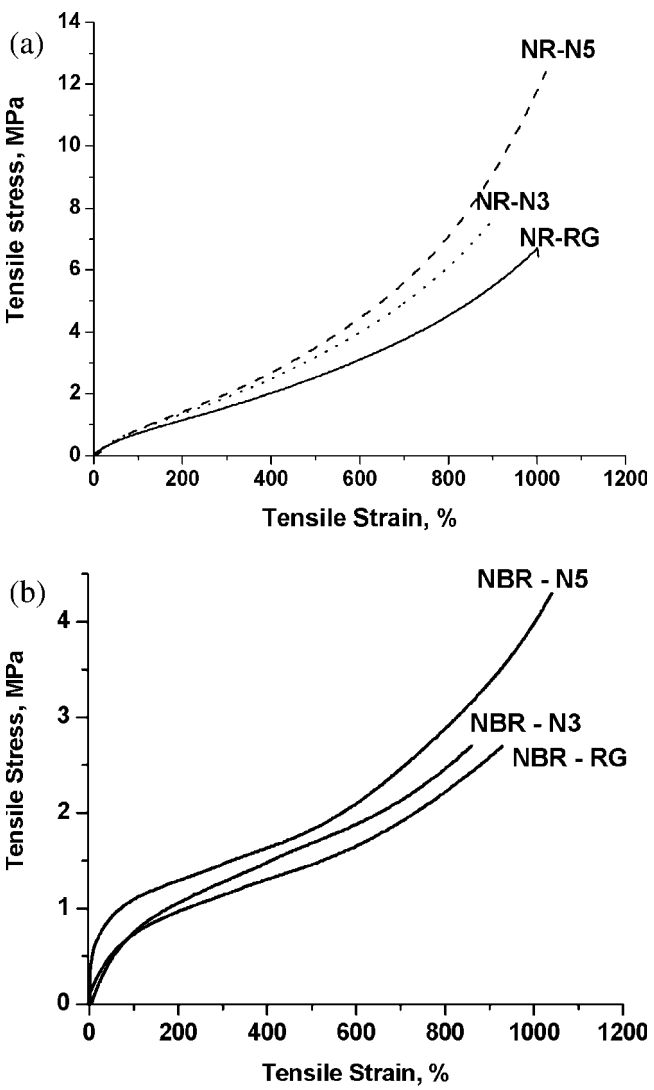

Figure 5 (a) Tensile stress–strain plots for NR vulcanizates, (b) tensile stress–strain plots for NBR vulcanizates.

TABLE V
Mechanical Properties of NR Vulcanizates

Compound	Tensile strength (MPa)	Elongation at break (%)	Modulus (MPa)		
			100%	200%	300%
NR-RG	6.7 ± 0.1	1000 ± 10	0.72 ± 0.01	1.15 ± 0.01	1.57 ± 0.02
NR-N3	7.6 ± 0.1	900 ± 10	0.83 ± 0.02	1.36 ± 0.03	1.89 ± 0.01
NR-N5	12.7 ± 0.2	1050 ± 20	0.81 ± 0.01	1.36 ± 0.02	1.92 ± 0.03

time exhibit only a marginal variation, the cure rate index of NR-N3 and NR-N5 do not vary to a remarkable extent.

Nitrile rubber. The cure curves are shown in Figure 4(b) and the cure parameters are tabulated in Table IV. About 18 and 14% increase in maximum torque value is observed for ZnO nanoparticle loaded compounds at 5 and 3 phr loading, respectively, in comparison with the conventional rubber grade ZnO. The results follow the similar trend as NR. An improvement in the $M_h - M_l$ value by 18% is observed for NBR-N5 and 13% for NBR-N3 in comparison with NBR-RG. There is a marginal change in the cure rate index for the vulcanizates containing ZnO nanoparticles in comparison with the vulcanizates containing conventional rubber grade ZnO, but no specific trend is observed.

Mechanical properties

Natural rubber. The tensile stress–strain plots are shown in Figure 5(a) and the results are tabulated in Table V. The tensile strength is observed to improve by 80% for NR-N5 and by 12% for NR-N3 in comparison with NR-RG. The elongation at break remains almost unaltered on the substitution of conventional ZnO with ZnO nanoparticles. Thus, ZnO nanoparticles improve the tensile strength of the vulcanizates without altering the elongation at break. The modulus at 300% also shows a remarkable improvement by 20% both for NR-N5 and NR-N3 in comparison to NR-RG. The improvement in the mechanical properties may be attributed to the increase in crosslink density, as discussed later, and better dispersion and increased interfacial interaction because of the reduction in size and increase in surface area.

Nitrile rubber. The tensile stress–strain plots are shown in Figure 5(b) and the results are tabulated in Table VI. Tensile strength shows an improvement by 70% for NBR-N5 and 12% increment for NBR-N3 in comparison with NBR-RG. There is no systematic trend of elongation at break, but it shows a marginal improvement for ZnO nanoparticles in comparison with conventional rubber grade ZnO at 5 phr loading. The modulus at 300% improves by $\sim$ 30 and 15% for NBR-N5 and NBR-N3, respectively, in comparison with NBR-RG. The results follow almost similar trend as NR.

Dynamic mechanical properties

Natural rubber. The plot of tan δ versus temperature is shown in Figure 6(a). The variation of E' with temperature is displayed as inset in the same figure. The results are tabulated in Table VII. There is a shift in T_g by 6°C for NR-N5 in comparison with NR-RG, which indicates an increase in crosslink density for the vulcanizates with ZnO nanoparticles. Tan δ at T_g is reduced from 2.05 to 1.95, indicating better reinforcement. It further supports the improvement in mechanical properties. The storage modulus at room temperature (25°C) shows an improvement of 15% with the use of ZnO nanoparticles as cure activator.

Nitrile rubber. The temperature dependencies of storage modulus and tan δ are depicted in Figure 6(b) and the results are tabulated in Table VIII. The results follow a similar trend as NR, the vulcanizate containing ZnO nanoparticles exhibiting a shift in T_g by 4 and 9°C in comparison with the vulcanizate containing conventional rubber grade ZnO and raw

TABLE VI
Mechanical Properties of NBR Vulcanizates

Compound	Tensile strength (MPa)	Elongation at break (%)	Modulus (MPa)		
			100%	200%	300%
NBR-RG	2.5 ± 0.2	930 ± 20	0.73 ± 0.01	0.97 ± 0.03	1.14 ± 0.02
NBR-N5	4.3 ± 0.3	1040 ± 10	1.10 ± 0.01	1.29 ± 0.01	1.46 ± 0.02
NBR-N3	2.8 ± 0.3	860 ± 20	0.75 ± 0.03	1.06 ± 0.02	1.28 ± 0.03

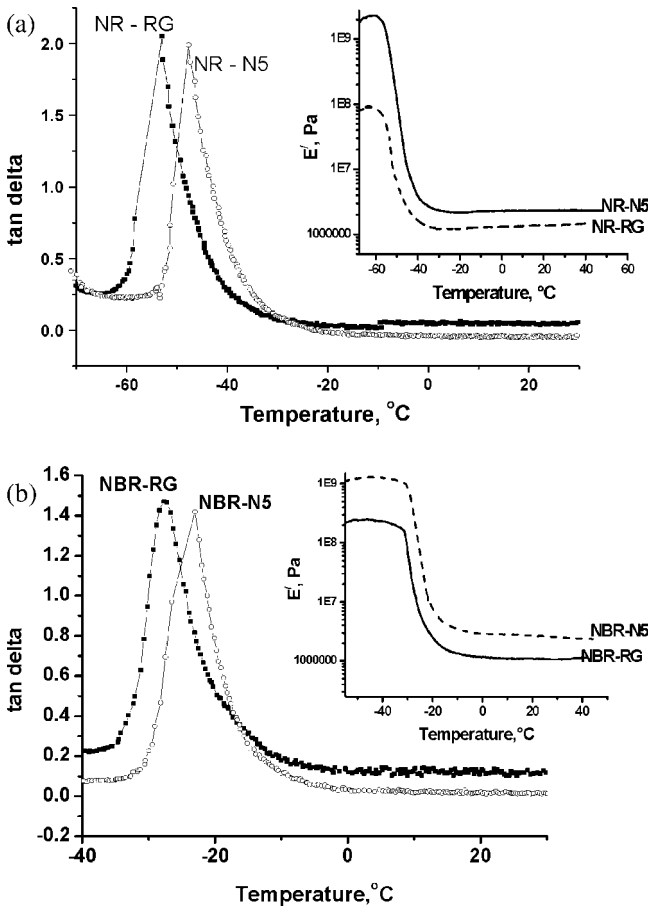

Figure 6 (a) Plot of tan δ versus temperature for NR vulcanizates (Inset: Plot of storage modulus versus temperature). (b) Plot of tan δ versus temperature for NBR vulcanizates (Inset: Plot of storage modulus versus temperature).

rubber, respectively. The storage modulus at room temperature is almost twice, on the substitution of conventional rubber grade ZnO by ZnO nanoparticles. It indicates that the crosslink density, as described later, increases with the incorporation of ZnO nanoparticles.

To further study the effect of cure activator, 5 phr of rubber grade ZnO was added to neat NBR and dynamic mechanical properties were studied on this unvulcanized sample. T_g and tan δ_{max} (−31°C and 1.68, respectively,) of this composite remain almost same as those of raw NBR (−32°C and 1.63, respectively). There is slight decrease in storage modulus of this composite over that of the raw rubber in the rubbery region. An almost similar result is obtained when NR and a mixture of NR with 5 phr conventional grade ZnO are compared. It means that only ZnO particles do not act as reinforcing fillers. It helps to increase the state of cure during vulcanization by acting as cure activator.

TABLE VII
Dynamic Mechanical Properties of NR Vulcanizates

Compound designation	Tan δ at T_g	Storage modulus at 25°C (MPa)	T_g (°C)
Neat NR	2.70	0.98	−66.0
NR-RG	2.05	2.25	−53.0
NR-N5	1.95	2.58	−47.0

TABLE VIII
Dynamic Mechanical Properties of NBR Vulcanizates

Compound designation	Tan δ at T_g	Storage modulus at 25°C (MPa)	T_g (°C)
Neat NBR	1.62	1.04	−32.0
NBR-RG	1.46	1.07	−27.0
NBR-N5	1.45	2.52	−23.0

Swelling studies

The SR and volume fraction of rubber in swollen gel for NR and NBR vulcanizates are listed in Tables IX and X respectively. The SR is observed to decrease by 18% for NR-N5 and 11% for NR-N3 in comparison with NR-RG and the volume fraction of rubber (V_r) increases by 40% for NR-N5 and by 16% for NR-N3 in comparison with NR-RG. The results further support the improvement in mechanical properties. Similar observations are made in the case of NBR also. The SR is seen to decrease by 15 and 10% for NBR-N5 and NBR-N3, respectively, in comparison with NBR-RG. The V_r values show an increment by 23% and 13% for NBR-N5 and NBR-N3 respectively, in comparison with NBR-RG.

Thus, the observations made in swelling studies further support the improvement in maximum torque value, mechanical and dynamic mechanical properties. Due to reduction in dimension of the ZnO nanoparticles, these effectively form the activation complex with sulfur accelerator and rubber, as shown in Scheme 1, during the vulcanization reaction. This leads to the formation of an increased number of vulcanization precursors, which further results in the formation of increased number of crosslinks that is supported by the decrease in SR and increase in V_r values. In addition, there will be increased interfacial interaction because of smaller size of the ZnO particles.

TABLE IX
Swelling Ratio and Volume Fraction of Rubber in the Swollen Gel for NR Vulcanizates

Compound	Swelling ratio	Volume fraction of rubber in the swollen gel (V_r)
NR-RG	3.06 ± 0.02	0.275 ± 0.005
NR-N5	2.50 ± 0.01	0.398 ± 0.003
NR-N3	2.70 ± 0.02	0.321 ± 0.005

TABLE X
Swelling Ratio and Volume Fraction of Rubber in the Swollen Gel for NBR Vulcanizates

Compound	Swelling ratio	Volume fraction of rubber in the swollen gel (V_r)
NBR-RG	2.30 ± 0.01	0.459 ± 0.005
NBR-N5	2.00 ± 0.03	0.567 ± 0.006
NBR-N3	2.08 ± 0.01	0.522 ± 0.007

CONCLUSIONS

Zinc oxide (ZnO) nanoparticles in the size range of 30–70 nm were synthesized by homogeneous precipitation and calcination method. The following observations were made when ZnO nanoparticles were used as cure activator instead of conventional rubber grade ZnO in NR and NBR formulations.

1. The maximum torque value was observed to increase by ~ 12% for NR and ~ 18% for NBR at 5 phr loading of ZnO nanoparticles.
2. The tensile strength showed a substantial improvement of 80% for NR and 70% for NBR. The modulus value at 300% elongation was observed to enhance by 20% for NR and 30% for NBR at 5 phr loading of ZnO nanoparticles.
3. The storage modulus increased by 15 and 130% for ZnO nanoparticles filled NR and NBR, respectively, as compared with conventional ZnO filled compounds.
4. The T_g was observed to be shifted by 6°C for NR and 4°C for NBR to higher temperature, which indicated an improvement in crosslink density.
5. The SR was observed to decrease both for NR and NBR along with an increase in V_r values, a measure of crosslinking density.
6. ZnO nanoparticles can be used to reduce the amount of ZnO in conventional formulations.

References

1. Morton, M. Introduction to Rubber Technology; Reinhold: New York, 1959.
2. George, W. Handbook of Fillers, 2nd ed.; William Andrew: Toronto, 1999.
3. Coran, A. Y. Science and Technology of Rubber; Eirich, F. R., Ed.; Academic Press: New York, 1978; p 291.
4. Tyer, G.; Helm, J. G. U.S. Pat. 6,066 (1849).
5. Review of Risks from metals in the UK; Presented at Chemicals Stakeholder Forum CSF/03/68, Fourteenth meeting 16 December 2003.
6. Gao, P. X.; Lao, C. S.; Hughes, W. L.; Wang, Z. L. J Chem Phys Lett 2005, 408, 174.
7. Hu, Z.; Oskam, G.; Lee, R.; Penn, I.; Pesika, N.; Searson, P. C. Phys Chem B 2003, 107, 3124.
8. Wong, E. M.; Bonevich, J. E.; Searson, P. C. J Phys Chem B 1998, 102, 7770.
9. Bahnemann, D. W.; Kormann, C.; Hoffmann, M. R. J Phys Chem 1987, 91, 3789.
10. Spanhel, L.; Anderson, M. A. J Am Chem Soc 1991, 113, 2833.
11. Hu, Z.; Chen S.; Peng, S. J Colloid Interface Sci 1996, 182, 457.
12. Inubushi, Y.; Takami, R.; Iwasaki, M.; Tada, H.; Ito, S. J Colloid Interface Sci 1998, 200, 220.
13. Wegner, G. Chem Mater 1998, 10, 460.
14. Guo, L.; Yang, S.; Yang, C.; Yu, P.; Wang, J.; Ge, W.; Wong, G. K. L. Appl Phys Lett 2000, 76, 2901.
15. Taubert, A.; Glasser, G.; Palms, D. Langmuir 2002, 18, 4488.
16. Kaneko, D.; Shouji, H.; Kawai, T.; Kon-No, K. Langmuir 2000, 16, 4086.
17. Carnes, C. L.; Klabunde, K. J. Langmuir 2000, 16, 3764.
18. Rodrıguez-Paez, J. E.; Caballero, A. C.; Villegas, M.; Moure, C.; Duran, P.; Fernandez, J. F. J Eur Ceram Soc 2001, 21, 925.
19. Zou, B. S.; Volkov, V. V.; Wang, Z. L. Chem Mater 1999, 11, 3037.
20. Lu, C. H.; Yeh, C. H. Mater Lett 1997, 33, 129.
21. Zhao, X. Y.; Zheng, B. C.; Li, C. Z.; Gu, H. C. Powder Technol 1998, 100, 20.
22. Milosevic, O.; Gagic, V.; Vodnik, J.; Mitrovic, A.; Karanovic, L.; Stojanovic, B.; Živkovic, L. Thin Solid Films 1997, 44, 296.
23. Kang, Y. C.; Park, S. B. J Mater Sci Lett 1997, 16, 131.
24. Li, W. J.; Shi, E. W.; Tian, M. Y.; Wang, B. G.; Zhong, W. Z. J Mater Res 1999, 14, 1532.
25. Li, W. J.; Shi, E. W.; Tian, M. Y.; Wang, B. G.; Zhong, W. Z. Sci Chin Ser E 1998, 44, 449.
26. Li Zhang, X. G. Colloid Surface Physicochem Eng Aspect 2003, 35, 226.
27. El-Shall, M. S.; Graiver, D.; Pernisz, U.; Baraton, M. I. Nanostruct Mater 1995, 6, 297.
28. Ray, S. S.; Okamoto, M. Prog Polym Sci 2003, 28, 1539.
29. Krishnamoorti, R.; Vaia, R. A., Eds. Polymer Nanocopmposites, Synthesis, Characterization and Modeling, ACS symposium series; American Chemical Society: Washington, DC, 2001.
30. Wen, J.; Wilkes, G. L. Chem Mater 1996, 8, 1667.
31. Mark, J. E. Polym Eng Sci 1996, 36, 2905.
32. Mark, J. E.; Jiang, C. Y.; Tang, M. Y. Macromolecules 1984, 17, 2613.
33. Bandyopadhyay, A.; Bhowmick, A. K.; Sarkar, M. D. J Appl Polym Sci 2004, 93, 2579.
34. Bandyopadhyay, A.; De Sarkar, M.; Bhowmick, A. K. Rubber Chem Technol 2004, 77, 830.
35. Sadhu, S.; Bhowmick, A. K. Rubber Chem Technol 2003, 76, 0860.
36. Sadhu, S.; Bhowmick, A. K. J Polym Sci Part B: Polym Phys 2004, 42, 1573.
37. Maiti, M.; Sadhu, S.; Bhowmick, A. K. J Polym Sci Part B: Polym Phys 2004, 42, 4489.
38. Hamed, G. R.; Hua, K. C. Rubber Chem Technol 2004, 77, 214.
39. Sahoo S.; Bhowmick, A. K. J Appl Polym Sci, to appear.
40. Morton, M. In Rubber Technology; Stephens, H. L., Ed.; Van Nostrand Reinhold: New York, 1987.
41. Wang, J.; Gao, L. Inorg Chem Commun 2003, 6, 877.
42. Bhowmick, A. K. Ph.D. Thesis, Indian Institute of Technology, Kharagpur, India, 1980.
43. http://www.shef.ac.uk/materials/about/facilities/x-raydiffraction/analysis.html. Access date 10th January 2006.
44. Klug, H. P.; Alexandar, L. E. X-Ray Diffraction Procedures for Polycrystalline and Amorphous Materials; Wiley: New York, 1962.